Chapter 7

SYNTHESES AND SPECTRAL ASPECTS OF CADMIUM(II) CHELATES DERIVED FROM ONS DONOR THIOSEMICARBAZONES

Contents

7.1. Introduction

Cadmium is a soft, malleable, ductile, bluish-white divalent metal and it prefers +2 oxidation state in most of its compounds. The average concentration of cadmium in the earth's crust is between 0.1 and 0.5 parts per million (ppm). Although cadmium has no known biological function in higher organisms, a cadmium-dependent carbonic anhydrase has been found in marine diatoms. Cadmium is used as a barrier to control neutrons in nuclear fission [1]. In molecular biology, cadmium is used to block voltage-dependent calcium channels from fluxing calcium ions, as well as in hypoxia research to stimulate proteasome-dependent degradation of Hif-1α [2].

Cadmium is an extremely toxic element that is naturally present in the environment and also as a result of human activities. There is substantial interest in the coordination chemistry of cadmium complexes because of the toxic environmental impact of cadmium. The mobilization and immobilization of cadmium in the environment, in organisms and in

some technical processes (such as in ligand exchange chromatography) have been shown to depend significantly on the complexation of the metal center by chelating nitrogen donor ligands [3]. Complexes of Cd(II) with different molecular architectures with the same trimesate ligands showing strong fluorescence have been reported [4]. Though cadmium has been known as a toxic metal and is often associated with mercury and lead as one of the biologically harmful metal ions, the cadmium(II) ion has recently been found to serve as the catalytic center in a newly discovered carbonic anhydrase [5].

Thiosemicarbazones and their complexes have been subject of interest in numerous studies because of their chemical and biological activities and they possess a wide range of beneficial medicinal properties that are often attributed to their chelating ability with metal ions. Complexes of Group 12 metals, zinc and cadmium, can provide an interesting range of stoichiometries depending on the preparative salts [6]. Here we discuss the syntheses and spectral characterization of cadmium(II) complexes of the aldehyde based ONS donor thiosemicarbazones.

7.2. Experimental

7.2.1. Materials

Cadmium(II) acetate dihydrate (E-Merck), 1,10-phenanthroline (phen), 2,2′-bipyridine (bipy), 4,4′-dimethyl-2,2′-bipyridine (4,4′-dmbipy), 5,5′-dimethyl-2,2′-bipyridine (5,5′-dmbipy) were used as received.

7.2.2. Syntheses of the thiosemicarbazones

The syntheses of thiosemicarbazones H_2L^1 and H_2L^2 are discussed already in Chapter 2.

7.2.3. Syntheses of the complexes

7.2.3.1. $[(CdL^1)_2]$ (26)

This complex was synthesized by refluxing a solution of H_2L^1 (0.190 g, 0.5 mmol) in 1:1 (v/v) mixture of DMF and methanol with a methanolic solution of $Cd(OAc)_2{\cdot}2H_2O$ (0.133 g, 0.5 mmol) for 3 hours. The complex formed was filtered, washed with methanol and dried *in vacuo*.

Elemental Anal. Found (Calcd.) (%) : C, 37.15 (36.72); H, 2.66 (2.47); N, 8.67 (8.56); S, 5.99 (6.54). Yield: 63%

7.2.3.2. $[CdL^1phen]$ (27)

Methanolic solution of cadmium(II) acetate dihydrate (0.133 g, 0.5 mmol) was added to a stirred mixture of H_2L^1 (0.190 g, 0.5 mmol) in DMF and methanol (1:1 v/v) and 1,10-phenanthroline (0.099 g, 0.5 mmol) in methanol. The resultant homogenous yellow solution was refluxed for three hours. The yellow product obtained was filtered, washed with methanol and dried *in vacuo*.

Elemental Anal. Found (Calcd.) (%) : C, 48.37 (48.34); H, 2.75 (3.00); N, 10.80 (10.44); S, 4.51 (4.78). Yield: 68%

7.2.3.3. [CdL^{1}bipy] (28)

To a stirred mixture of H_2L^1 (0.190 g, 0.5 mmol) in DMF and methanol (1:1 v/v) and 2,2′-bipyridine (0.078 g, 0.5 mmol) in methanol, cadmium(II) acetate dihydrate (0.133 g, 0.5 mmol) was added. The resultant yellow solution was refluxed for 3 hours and the yellow product separated out was filtered, washed with methanol and dried *in vacuo*.

Elemental Anal. Found (Calcd.) (%) : C, 46.35 (46.42); H, 3.24 (3.12); N, 10.70 (10.83); S, 4.75 (4.96). Yield: 74%

7.2.3.4. [CdL^1(4,4′-dmbipy)] (29)

To a stirred mixture of H_2L^1 (0.190 g, 0.5 mmol) in DMF and methanol (1:1 v/v) and 4,4′-dimethyl-2,2′-bipyridine (0.092 g, 0.5 mmol) in methanol, methanolic solution of cadmium(II) acetate dihydrate (0.133 g, 0.5 mmol) was added. The resultant yellow solution was refluxed for 3 hours and the yellow product separated out was filtered, washed with methanol and dried *in vacuo*.

Elemental Anal. Found (Calcd.) (%) : C, 48.30 (48.05); H, 3.89 (3.58); N, 10.26 (10.38); S, 4.84 (4.75). Yield: 60%

7.2.3.5. [CdL^1(5,5′-dmbipy)] (30)

Methanolic solution of cadmium(II) acetate dihydrate (0.133 g, 0.5 mmol) was added to a stirred mixture of H_2L^1 (0.190 g, 0.5 mmol) in DMF and methanol (1:1 v/v) and 5,5′-dimethyl-2,2′-bipyridine (0.092 g, 0.5 mmol) in methanol. The resultant yellow solution was refluxed for three hours. The yellow product obtained was filtered, washed with methanol and dried *in vacuo*.

Elemental Anal. Found (Calcd.) (%) : C, 48.34 (48.05); H, 3.25 (3.58); N, 10.87 (10.38); S, 4.51 (4.75). Yield: 62%

7.2.3.6. [$(CdL^2)_2$] (31)

This complex was synthesized by refluxing a solution of H_2L^2 (0.193 g, 0.5 mmol) in 1:1 (v/v) mixture of DMF and methanol with a methanolic solution of $Cd(OAc)_2{\cdot}2H_2O$ (0.133 g, 0.5 mmol) for 3 hours. The complex formed was filtered, washed with methanol and dried *in vacuo*.

Elemental Anal. Found (Calcd.) (%) : C, 36.59 (36.27); H, 3.82 (3.65); N, 8.55 (8.46); S, 6.47 (6.46). Yield: 60%

7.2.3.7. [CdL^2phen] (32)

Methanolic solution of cadmium(II) acetate dihydrate (0.133 g, 0.5 mmol) was added to a stirred mixture of H_2L^2 (0.193 g, 0.5 mmol) in DMF and methanol (1:1 v/v) and 1,10-phenanthroline (0.099 g, 0.5 mmol) in methanol. The resultant homogenous yellow solution was refluxed for three hours. The yellow product obtained was filtered, washed with methanol and dried *in vacuo*.

Elemental Anal. Found (Calcd.) (%) : C, 47.64 (47.91); H, 3.61 (3.87); N, 10.44 (10.35); S, 4.56 (4.74). Yield: 67%

7.2.3.8. [CdL^2bipy] (33)

To a stirred mixture of H_2L^2 (0.193 g, 0.5 mmol) in DMF and methanol (1:1 v/v) and 2,2′-bipyridine (0.078 g, 0.5 mmol) in methanol, cadmium(II) acetate dihydrate (0.133 g, 0.5 mmol) was added. The resultant yellow

solution was refluxed for 3 hours and the yellow product separated out was filtered, washed with methanol and dried *in vacuo*.

Elemental Anal. Found (Calcd.) (%) : C, 45.78 (45.99); H, 4.14 (4.01); N, 10.58 (10.73); S, 4.78 (4.91). Yield: 69%

7.3. Results and discussion

We synthesized and characterized eight cadmium complexes which are found to be stable. The complexes are soluble in organic solvents like DMF and DMSO. The thiosemicarbazones coordinate to the central metal ion in the thioiminolate form in all the complexes as evidenced by the IR spectral data. Compounds $[(CdL^{1})_2]$ (**26**) and $[(CdL^{2})_2]$ (**31**) are dimeric in nature while others are monomeric mixed ligand metal chelates. The isolation of X-ray quality single crystals of the Cd(II) complexes had not been successful. The synthesized complexes are characterized by the following physico-chemical methods.

7.3.1. Elemental analyses

Elemental analyses data of complexes **26** and **31** reveal that metal and thiosemicarbazone are in the ratio 1:1 and in all other complexes the metal, thiosemicarbazone and the respective heterocyclic bases are in the ratio 1:1:1.

7.3.2. Molar conductivity

The molar conductivity of the complexes in DMF (10^{-3} M) were measured at 298 K with a Systronic model 303 direct reading conductivity bridge, which suggest that these complexes are non-electrolytic in nature [7].

Table 7.1. Molar conductivity of Cd(II) complexes

Compound	λ_m[a]
$[(CdL^1)_2]$ (**26**)	3.4
$[CdL^1phen]$ (**27**)	2.0
$[CdL^1bipy]$ (**28**)	2.5
$[CdL^1(4,4'\text{-dmbipy})]$ (**29**)	3.6
$[CdL^1(5,5'\text{-dmbipy})]$ (**30**)	2.6
$[(CdL^2)_2]$ (**31**)	3.5
$[CdL^2phen]$ (**32**)	4.0
$[CdL^2bipy]$ (**33**)	3.3

[a] = mho cm^2 mol^{-1}

7.3.3. Infrared spectra

The IR spectra of the thiosemicarbazones when compared with the Cd(II) complexes confirm the coordination of the thiosemicarbazone to the metal. The significant bands observed in the IR spectra of the thiosemicarbazones and their complexes are summarized in Table 7.2.

The band corresponding to azomethine bond, ν(C=N), shifts to higher energy on complexation due to the combination of ν(C=N) with the newly formed C=N bond which results from the loss of the thioamide hydrogen from the thiosemicarbazone moiety [8-12]. Strong bands found at 1071 and 1067 cm^{-1} in the thiosemicarbazones are assigned to the ν(N–N) band. The increase in frequency of this band in the spectra of complexes is due to the increase in the bond strength, again confirming the coordination *via* the azomethine nitrogen. Coordination *via* thioiminolate sulfur is indicated by the downward shift of frequencies of δ/ν CS bands in the

complexes [13]. Some of the IR spectra of complexes are given in Figs. 7.1-7.6.

Table 7.2. IR spectral assignments (cm^{-1}) of thiosemicarbazones and their Cd(II) complexes

Compound	ν(O–H)	ν(C=N)	ν(N=C)[a]	ν(N–N)	ν(C=S)/ν(C–S), δ(C=S)/δ(C–S)	ν(C–O)	ν(Cd–O)	ν(Cd–N)
H_2L^1	3441	1540	----	1071	1333, 857	1267		----
$[(CdL^1)_2]$ (**26**)	----	1596	1546	1098	1288, 839	1228	464	431
$[CdL^1phen]$ (**27**)	----	1595	1550	1102	1309, 842	1228	465	422
$[CdL^1bipy]$ (**28**)	----	1599	1550	1100	1306, 844	1228	470	443
$[CdL^1(4,4'\text{-dmbipy})]$ (**29**)	----	1599	1550	1098	1316, 835	1237	463	427
$[CdL^1(5,5'\text{-dmbipy})]$ (**30**)	----	1598	1550	1100	1316, 840	1237	463	435
H_2L^2	3454	1539	----	1067	1342, 851	1257		----
$[(CdL^2)_2]$ (**31**)	----	1597	1556	1101	1328, 811	1225	472	459
$[CdL^2phen]$ (**32**)	----	1590	1560	1090	1330, 840	1230	466	446
$[CdL^2bipy]$ (**33**)	----	1586	1558	1092	1325, 833	1228	475	442

[a] = newly formed C=N bond

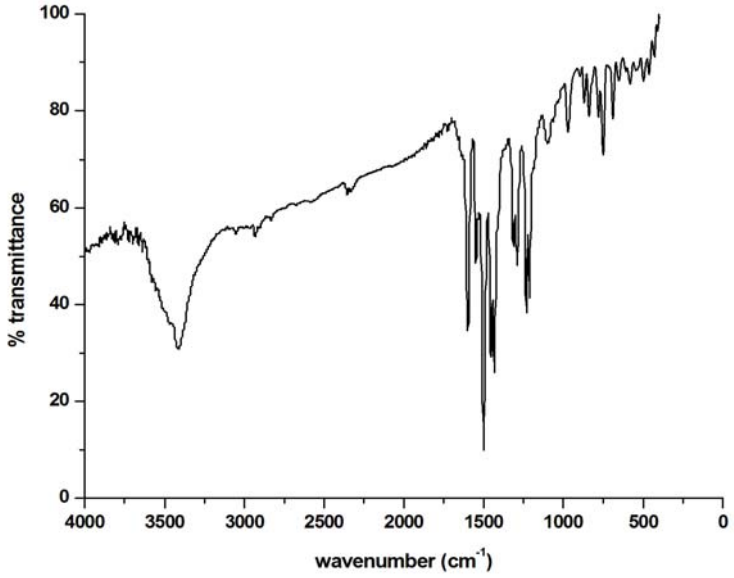

Fig. 7.1. Infrared spectrum of $[(CdL^1)_2]$ (26).

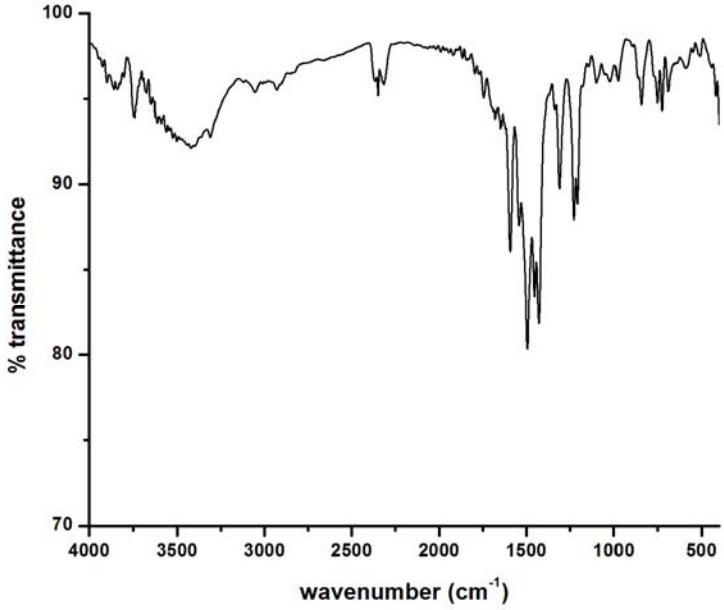

Fig. 7.2. Infrared spectrum of [CdL^{1}bipy] (28).

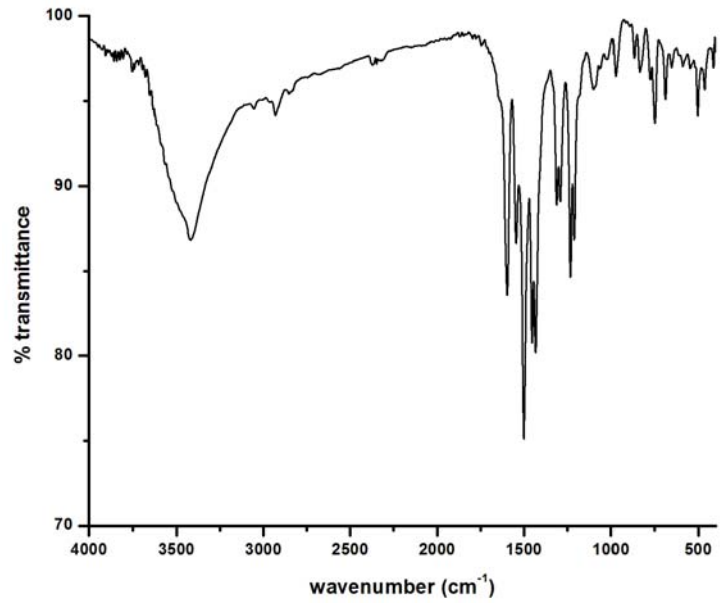

Fig. 7.3. Infrared spectrum of [CdL^1(4,4′-dmbipy)] (29).

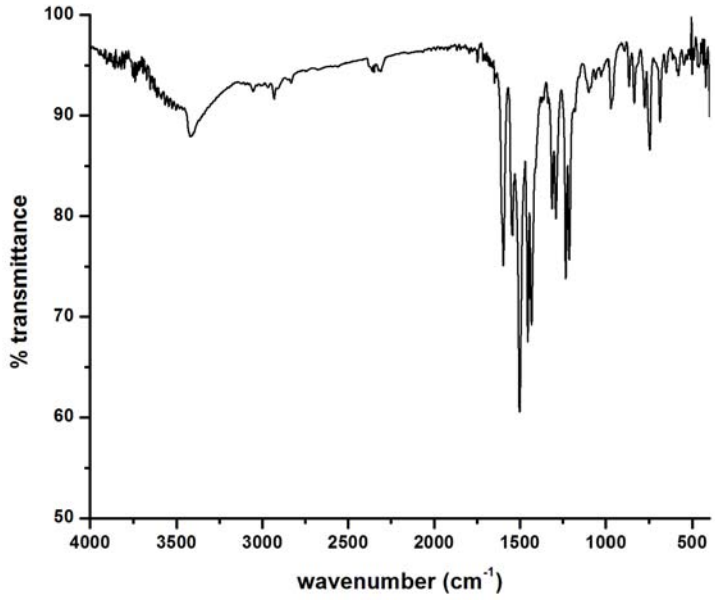

Fig. 7.4. Infrared spectrum of [CdL^1(5,5′-dmbipy)] (30).

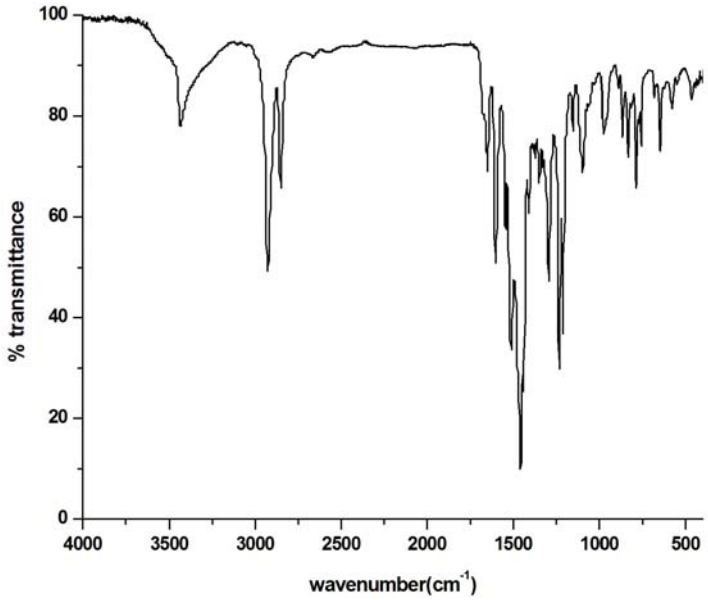

Fig. 7.5. Infrared spectrum of [CdL^{2}phen] (32).

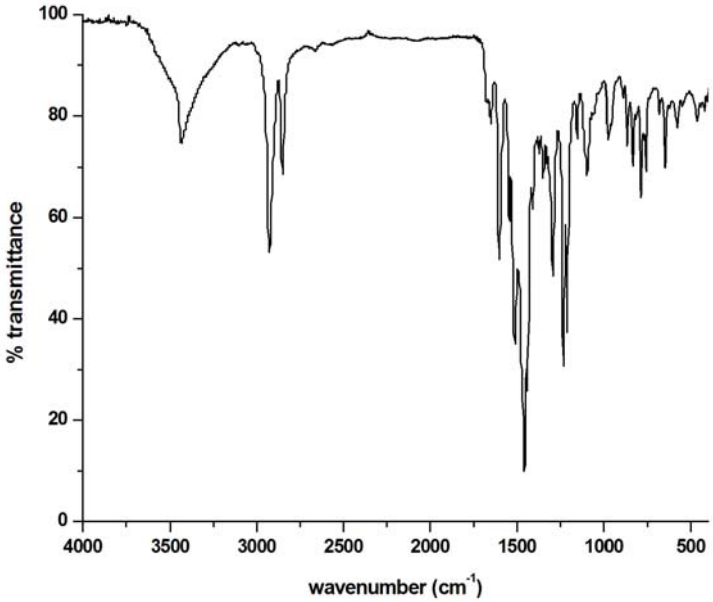

Fig. 7.6. Infrared spectrum of [CdL^{2}bipy] (33).

7.3.4. Electronic spectra

The electronic spectral assignments for the thiosemicarbazones and their Cd(II) complexes recorded in DMF are summarized in Table 7.3. The electronic spectra of the thiosemicarbazones showed bands in the range 28770-30490 cm^{-1} which are assignable to azomethine bond and the thiosemicarbazone moiety [14]. These bands are slightly shifted on complexation. In addition to these bands due to intraligand transitions, new bands around 24990-26110 cm^{-1} range are observed in the spectra of complexes. These bands can be assigned to metal to ligand charge transfer transitions. No appreciable absorptions occurred below 20000 cm^{-1}, indicating the absence of *d-d* bands, which is in accordance with the d^{10} configuration of Cd(II) ion [15]. The electronic spectra of complexes are given in Figs. 7.7 and 7.8.

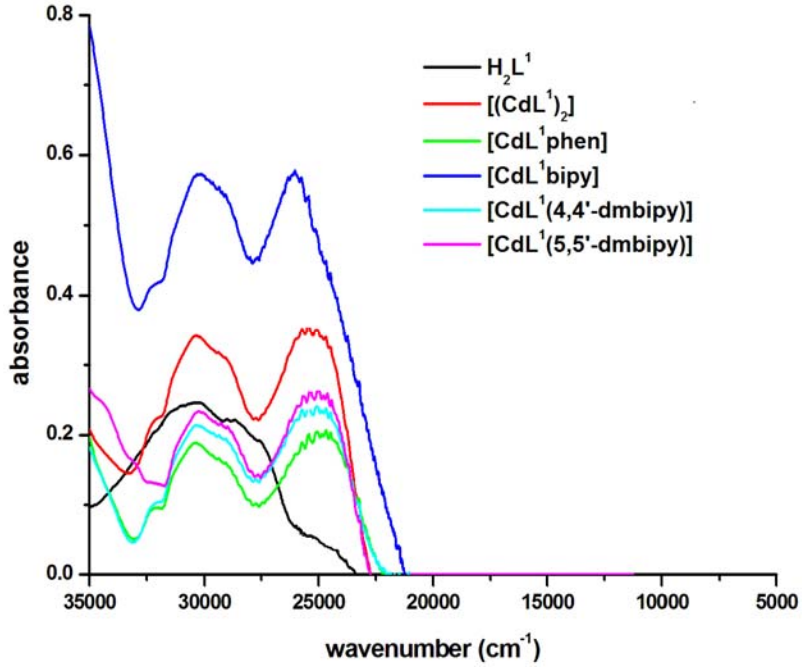

Fig. 7.7. Electronic spectra of H_2L^1 and its Cd(II) complexes.

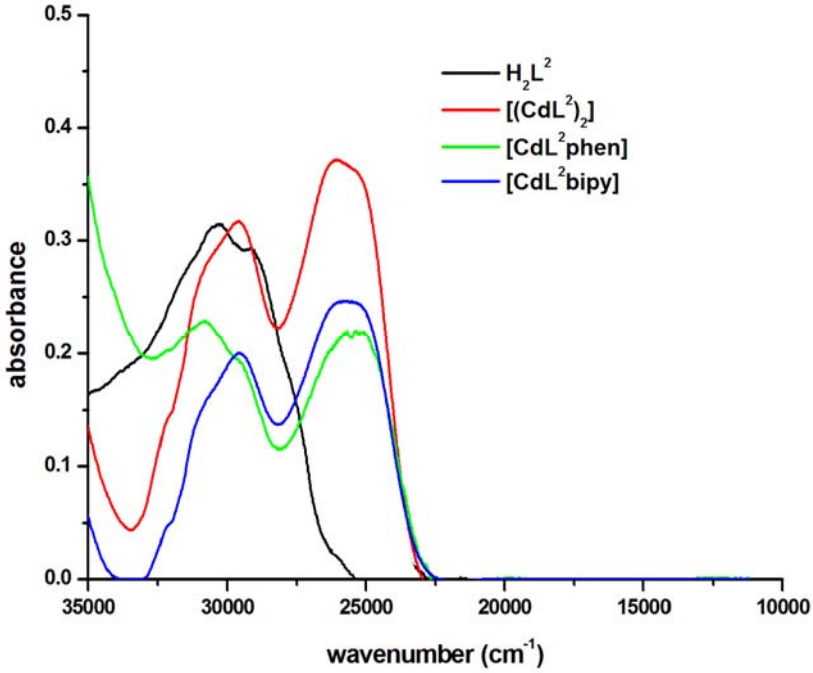

Fig. 7.8. Electronic spectra of H_2L^2 and its Cd(II) complexes.

Table 7.3. Electronic spectral assignments (cm^{-1}) of thiosemicarbazones and their Cd(II) complexes

Compound	n→π*/π→π*	LMCT
H_2L^1	28770, 30490	----
$[(CdL^1)_2]$ (**26**)	29210, 30380	25430
$[CdL^1phen]$ (**27**)	29030, 30450	24990
$[CdL^1bipy]$ (**28**)	29090, 30210	26110
$[CdL^1(4,4'\text{-dmbipy})]$ (**29**)	29250, 30330	25230
$[CdL^1(5,5'\text{-dmbipy})]$ (**30**)	29020, 30290	25160
H_2L^2	29300, 30490	----
$[(CdL^2)_2]$ (**31**)	29590, 30890	26050
$[CdL^2phen]$ (**32**)	29520, 30820	25550
$[CdL^2bipy]$ (**33**)	29520, 30700	25740

References

[1] G. Buxbaum, G. Pfaff, "Cadmium Pigments", Industrial inorganic pigments, Wiley-VCH, pp.121, 2005.

[2] K.R. Nambiar, "Helium-cadmium Laser", Lasers: Principles, Types and Applications, 2006.

[3] L. Pag, J.N. Lindner, G. Davies, D.E. Seitz, B.L. Karger, Anal. Chem. 51 (1979) 433.

[4] J.-C. Dai, X.-T. Wu, Z.-Y. Fu, C.-P. Cui, S.-M. Hu, W.-X. Du, L.-M. Wu, H.-H. Zhang, R.-Q. Sun, Inorg. Chem. 41 (2002) 1391.

[5] T.W. Lane, F.M.M. Morel, Proc. Natl. Acad. Sci. USA 97 (2000) 4627.

[6] E. Bermejo, A. Castineiras, L.M. Fostiak, I.G. Santos, J.K. Swearingen, D.X. West, Polyhedron 23 (2004) 2303.

[7] W.J. Geary, Coord. Chem. Rev. 7 (1971) 81.

[8] M. Joseph, V. Suni, M.R.P. Kurup, M. Nethaji, A. Kishore, S.G. Bhat, Polyhedron 23 (2004) 3069.

[9] M.A. Ali, M.T.H. Tarafdar, J. Inorg. Nucl. Chem. 39 (1977) 1785.

[10] M.J.M. Campbell, Coord. Chem. Rev. 15 (1975) 279.

[11] B.S. Garg, M.R.P. Kurup, S.K. Jain, Y.K. Bhoon, Transit. Met. Chem. 13 (1988) 247.

[12] B.S. Garg, M.R.P. Kurup, S.K. Jain, Y.K. Bhoon, Transit. Met. Chem. 16 (1991) 111.

[13] P.F. Rapheal, E. Manoj, M.R.P. Kurup, E. Suresh, Polyhedron 26 (2007) 607.

[14] A. Castineiras, E. Bermejo, D.X. West, L.J. Ackerman, J.V. Martinez, S.H. Ortega, Polyhedron 18 (1999) 1469.

[15] V. Philip, V. Suni, M.R.P. Kurup, Polyhedron 25 (2006) 1931.

Chapter 8

SYNTHESIS, CRYSTAL STRUCTURE AND SPECTRAL ASPECTS OF A DIOXIDOMOLYBDENUM(VI) CHELATE DERIVED FROM ONS DONOR THIOSEMICARBAZONE

Contents

8.1. Introduction

Molybdenum is a biologically important trace element which is of essential importance. It is required by enzymes catalyzing diverse key reactions in the global carbon, sulfur and nitrogen metabolism. It occurs in the redox-active sites of molybdoenzymes involved in nitrogen, sulfur or carbon metabolism [1]. The 'oxo-type' molybdoenzymes, which possess a common molybdenum cofactor, catalyze biological two electron reactions that involve a change in the number of oxygen atoms in the substrate [2]. The mononuclear molybdoenzymes contain terminal oxo group(s), believed to be obligatory for the oxotransferase activity of these enzymes. It occurs in a wide range of metalloenzymes in bacteria, fungi, algae, plants and animals where it forms part of the active sites of these enzymes. The active site includes the metal atom coordinated to one or two pyranopterin molecules and to a variable number of ligands such as oxygen, sulfur and selenium atoms [3,4].

Diverse class of molybdenum complexes were prepared, tested and developed for various pharmaceutical purposes, whereby their anticancer activities gained special attention. For example, tetrathiomolybdate (TM) is an anticopper drug under development for treating Wilson's disease. Its mechanism of action involves forming a tight tripartite complex in the blood with serum albumin and available copper. In addition, it has been shown that lowering copper levels with TM produces an antiangiogenic, anticancer effect, probably due to inhibition of many copper-dependent proangiogenic cytokines. Therefore, it has shown a promising role in suppressing tumor angiogenesis, retinal neovascularization and pathologic inflammatory conditions [5,6].

Additionally, polyoxometalates, negatively charged inorganic substances which contain early transition metal ions and make a cluster with the surrounding oxygen atoms are a large class of inorganic compounds with great molecular diversity and significant potential applications in chemistry and medicine [7]. Yamase had reported that significant antitumoral effect of polyoxomolybdates, especially $[NH_3Pr^i]_6[Mo_7O_{24}]\cdot 3H_2O$ (PM-8) was found against MX-1 murine mammary cancer cell line, Meth A sarcoma and MM46 adenocarcinoma [8]. √-octamolybdates containing aminoacids and peptides showed differential cell-growth inhibition in a close dependent manner selectively on hepatocellular carcinoma cell line (HepG2) and breast cancer cell line (MCF-7) [9]. Furthermore, metallocene diacido complexes containing molybdenum exhibit antitumor activity for a wide spectrum of murine and human tumors with reduced toxicity when compared with cisplatin [10].

Molybdenum is a versatile transition element because it possesses a large number of stable and accessible oxidation states as well as coordination numbers. The formal oxidation state of molybdenum fluctuates between +6 and +4 *via* a +5 intermediate during turnover [11]. Complexes containing the molybdenum-oxo group dominate the higher oxidation state of molybdenum. Most simple dioxidomolybdenum(VI) coordination complexes contain the *cis*-MoO_2^{2+} cation. The chemistry of nitrogen-sulfur chelating ligands bound to Mo with higher oxidation states is a field of great interest. Thiosemicarbazones obtained by condenzing ring substituted aromatic thiosemicarbazides with *o*-hydroxy carbonyl compounds have rarely been used in molybdenum chemistry. These ligands are of particular interest because their complexes of the type MoO_2L or MoOL possess one or two "open" coordination sites that can be utilized for substrate binding.

8.2. Experimental

8.2.1. Materials

The reagents used for the synthesis of the ligand H_2L^1 are discussed in Chapter 2. $MoO_2(acac)_2$ (Sigma-Aldrich) was used as received. Solvents used are methanol and dimethylformamide.

8.2.2. Synthesis of the thiosemicarbazone H_2L^1

The synthesis of thiosemicarbazone H_2L^1 is discussed already in Chapter 2.

8.2.3. Synthesis of the complex [MoO_2L^1DMF]·DMF (34)

This complex was synthesized by mixing a solution of H_2L^1 (0.190 g, 0.5 mmol) in a mixture of DMF and methanol (1:1 v/v) with a hot methanolic solution of $MoO_2(acac)_2$ (0.163 g, 0.5 mmol) and refluxing for 3 hours. This was cooled and the orange colored crystalline complex formed was filtered, washed with methanol and dried *in vacuo*.

Elemental Anal. Found (Calcd.) (%) : C, 38.20 (38.66); H, 4.16 (4.02); N, 10.81 (10.74); S, 5.40 (4.92). Yield: 57%

8.3. Results and discussion

The stoichiometric reaction of bis(acetylacetonato)dioxido molybdenum(VI) with H_2L^1 in a N,N-dimethylformamide-methanol binary mixture afforded the orange six coordinate complex [MoO_2L^1DMF]·DMF (**34**) even though the expected product was [(MoO_2L^1)$_2$]. The thiosemicarbazone H_2L^2 did not give any complex with molybdenum. We tried to prepare Mo(VI) complexes using heterocyclic bases like pyridine and γ–picoline with both the thiosemicarbazones H_2L^1 and H_2L^2. Unfortunately these bases are not getting coordinated to MoO_2^{2+}. Instead, the solvent DMF is found to coordinate to the metal in all the cases. The complex **34** is soluble in DMF and DMSO. It is characterized by the following physicochemical methods.

8.3.1. Elemental analysis

The analytical data indicate that the observed C, H, N and S values are in close agreement with that of the proposed formula [MoO_2L^1DMF]·DMF.

8.3.2. Molar conductivity and magnetic susceptibility measurements

The conductivity measurement was made in DMF (10^{-3} M) and the complex was found to be electrically non-conducting in solution [12]. Magnetic susceptibility data indicate that the complex is diamagnetic. λ_m = 10.2 $ohm^{-1}cm^2mol^{-1}$, μ_{eff} = 0.21 B.M.

8.3.3. Infrared spectrum

Table 8.1. lists the tentative assignments of the main IR bands of the dioxidomolybdenum(VI) complex in 4000-400 cm^{-1} region. The ligand H_2L^1 shows bands at 3441 and 3305 cm^{-1}, which are due to the stretching modes of the –OH and –^{2}NH groups respectively. These bands are absent in the complexes which suggests deprotonation of the phenolic group, indicating coordination through the phenolic oxygen and enolization of the thioamido sulfur followed by deprotonation. The ligand has a band at 1267 cm^{-1} which is due to ν(C–O). This band is shifted to 1253 cm^{-1} in the complex which also indicates the coordination of O^- [13]. The band corresponding to azomethine bond, ν(C=N), shifts to higher energy on coordination due to the combination of ν(C=N) with the newly formed C=N bond which results from the loss of the thioamide hydrogen from the thiosemicarbazone moiety [14-18]. The increase in frequency of ν(N–N) band in the complex, due to an increase in the bond strength, again confirms coordination *via* the azomethine nitrogen [19,20]. The decrease in frequency of the ν(CS) band from 1333 cm^{-1} in the thiosemicarbazone by 12 cm^{-1} upon complexation indicates coordination *via* the thioiminolato sulfur [21,22]. The complex exhibits two bands at 845 and 916 cm^{-1} assigned to symmetric and antisymmetric vibrations, respectively, of the *cis*-MoO_2^{2+} core [23,24].

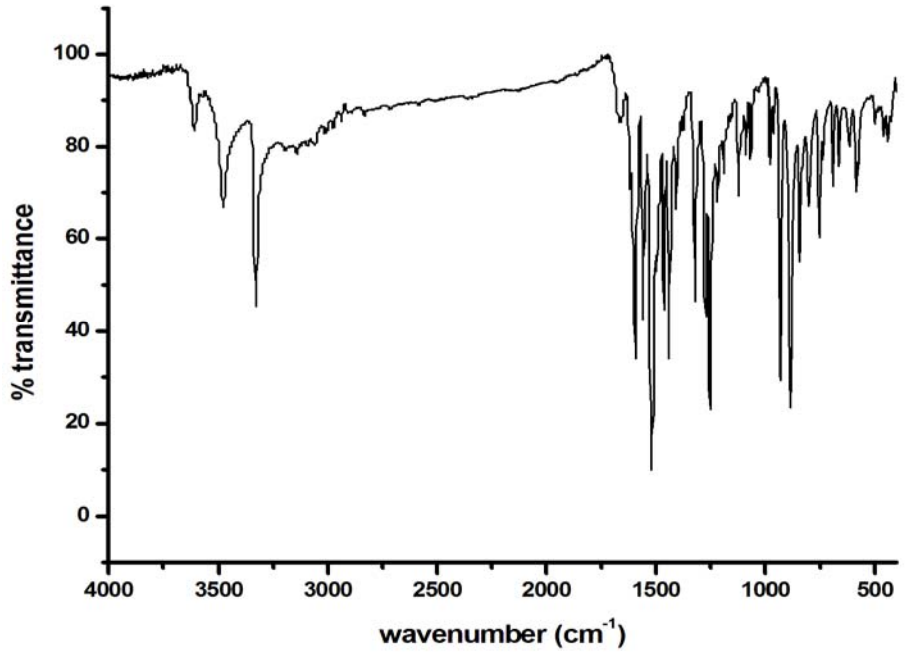

Fig. 8.1. Infrared spectrum of $[MoO_2L^1DMF]\cdot DMF$ (34).

Table 8.1. IR spectral assignments (cm^{-1}) of H_2L^1 and its dioxidomolybdenum(VI) complex

Compound	ν(O–H)	ν(C=N)	ν(C=N)[a]	ν(N–N)	ν(C=S)/ν(C–S), δ(C=S)/δ(C–S)	ν(C–O)	ν(Mo=O)
H_2L^1	3441	1540	----	1071	1333, 857	1267	----
$[MoO_2L^1DMF]\cdot DMF$ (**34**)	----	1590	1558	1122	1320, 804	1253	887, 935

[a] = newly formed C=N bond

8.3.4. Electronic spectrum

The electronic spectrum of the dioxidomolybdenum(VI) complex was recorded in DMF (10^{-3} M) and the electronic spectral assignments are given in Table 8.2. The thiosemicarbazone H_2L^1 shows bands at 30490 and 28770 cm^{-1} corresponding to intraligand transitions. These bands suffer marginal shifts upon complexation. The complex displays a broad band at 24330

cm^{-1} which is assignable to L → Mo (dπ) LMCT transition [25-27]. The electronic spectrum of the complex is given in Fig. 8.2.

Table 8.2. Electronic spectral assignments (cm^{-1}) of thiosemicarbazone and the Mo(VI) complex

Compound	n→π*/π→π*	LMCT	d-d
H_2L^1	28770, 30490	----	----
$[MoO_2L^1DMF]\cdot DMF$ (**34**)	28500, 30070	24330	----

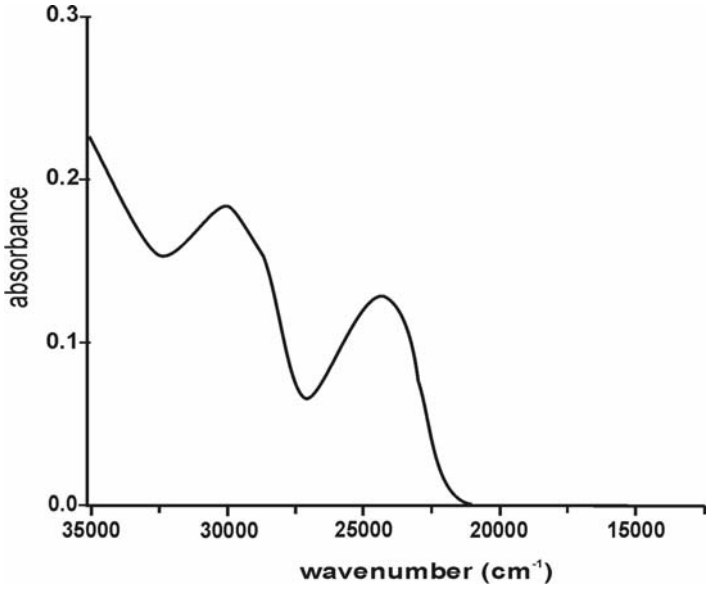

Fig. 8.2. Electronic spectrum of $[MoO_2L^1DMF]\cdot DMF$ (34).

8.3.5. X-ray crystallography

Single crystals of $[MoO_2L^1DMF]\cdot DMF$ (**34**) was obtained by slow evaporation of its mother liquor over a week. The crystallographic data and structure refinement parameters for the complex at 296 K are given in Table 8.3. An orange block shaped crystal with approximate dimensions of 0.30 × 0.25 × 0.20 mm^3 was selected for collecting the data. It was mounted on a Bruker SMART APEXII CCD diffractometer, equipped with a graphite crystal, incident-beam monochromator and a fine focus sealed tube with Mo Kα radiation (λ = 0.71073 Å) as the X-ray source. The unit cell dimensions were measured and the data collection was performed at 296 K. Bruker SMART software was used for data acquisition and Bruker SAINT software for data integration [28]. Absorption corrections were carried out using SADABS based on Laue symmetry using equivalent reflections [29]. The structure was solved by direct methods using SHELXS97 [30] and refined by full-matrix least-squares calculations with SHELXL97 software package [31]. The molecular and crystal structures were plotted using DIAMOND version 3.2g [32].

All non-hydrogen atoms were refined anisotropically and all H atoms on C were placed in calculated positions, guided by difference maps, with C–H bond distances 0.93–0.96 Å. H atoms were assigned as U_{iso}=1.2U_{eq} (1.5 for Me). The N3–H′ hydrogen atom was located from difference Fourier maps and the distance was restrained using DFIX instruction. The final refinement cycle was based on all 6488 independent reflections and 326 variables with R_1 = 0.0341, wR_2 = 0.0778.

Table 8.3 Crystal data and structure refinement parameters for complex 34

Parameters	$[MoO_2L^1DMF]\cdot DMF$ (**34**)
Empirical formula	$C_{21}H_{26}BrMoN_5O_6S$
Formula weight	652.38
Temperature	296 K
Wavelength	0.71073 Å
Crystal system	Monoclinic
Space group	$P2_1/n$
Unit cell dimensions	a = 15.4646(6) Å
	b = 11.0191(4) Å
	c = 15.4756(6) Å
	α = 90°
	β = 98.761(2)°
	γ = 90°
Volume	2606.37(17) $Å^3$
Z	4
Density (calculated)	1.663 Mg/m^3
Absorption coefficient	2.161 mm^{-1}
F(000)	1312
Crystal size	0.30 x 0.25 x 0.20 mm^3
θ range for data collection	2.28 to 28.31°
Limiting indices	$-20 \le h \le 20$
	$-14 \le k \le 14$
	$-20 \le l \le 20$
Reflections collected	44354
Independent reflections	6488 [R(int) = 0.0441]
Refinement method	Full-matrix least-squares on F^2
Data / restraints / parameters	6488 / 1 / 326
Goodness-of-fit on F^2	1.015
Final R indices [$I > 2\sigma(I)$]	R_1 = 0.0341, wR_2 = 0.0778
R indices (all data)	R_1 = 0.0540, wR_2 = 0.0862
Largest diff. peak and hole	1.485 and -1.308 e $Å^{-3}$

$R_1 = \Sigma||F_o| - |F_c|| \,/\, \Sigma|F_o|$

$wR_2 = [\Sigma w(F_o^2-F_c^2)^2 \,/\, \Sigma w(F_o^2)^2]^{1/2}$

This complex crystallizes into a monoclinic $P2_1/n$ space group. The molecular structure of the complex with the atom numbering scheme is shown in Fig. 8.3 and relevant bond distances and angles are presented in Table 8.4. The coordination geometry around molybdenum can be best described as distorted octahedral in which the thiosemicarbazone coordinates to the metal in a tridentate manner forming five membered and six membered metallocycles involving the MoO_2^{2+} moiety. Oxygen, nitrogen and sulfur atoms of the thiosemicarbazone and one of the terminal oxo atom occupy the equatorial positions of the complex. The axial positions are occupied by the other terminal oxygen and oxygen atom of the solvent N,N-dimethylformamide. The principal ligand is bonded to *cis*-MoO_2^{2+} in a planar fashion, coordinating through the nitrogen N(1), sulfur S(1) and oxygen O(2) atoms. The large Mo(1)–O(5) distance reveals that O atom of the solvent dimethylformamide is rather weakly coordinated to the MoO_2^{2+} core.

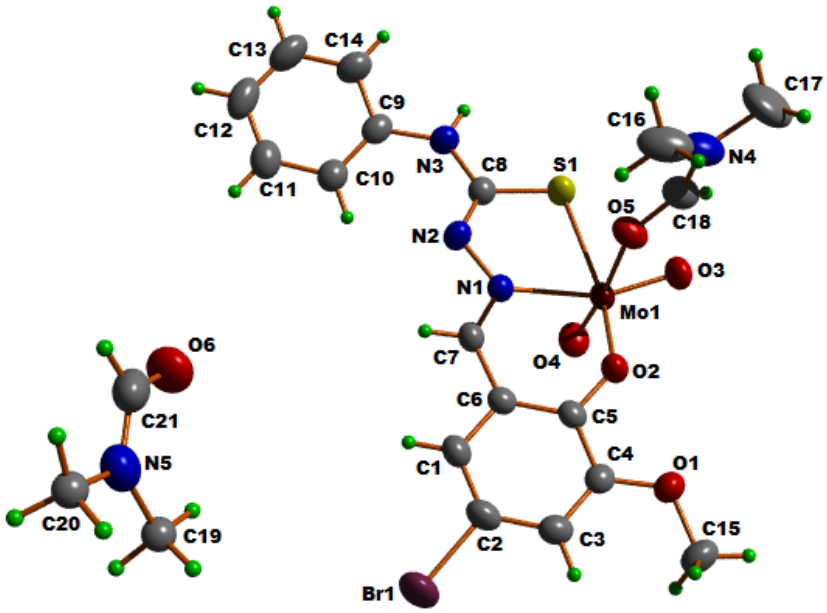

Fig. 8.3. Structure and labelling diagram for $[MoO_2L^1DMF]\cdot DMF$ (34).

Table 8.4 Selected bond lengths and angles for complex 34

Bond lengths (Å)		Bond angles (°)	
Mo(1)–S(1)	2.4549(8)	S(1)–Mo(1)–O(2)	152.66(6)
Mo(1)–O(2)	1.939(1)	S(1)–Mo(1)–O(3)	89.23(7)
Mo(1)–O(3)	1.699(1)	S(1)–Mo(1)–O(4)	97.86(8)
Mo(1)–O(4)	1.690(2)	S(1)–Mo(1)–O(5)	81.68(5)
Mo(1)–N(1)	2.250(2)	S(1)–Mo(1)–N(1)	75.39(6)
Mo(1)–O(5)	2.370(2)	O(2)–Mo(1)–O(3)	106.43(9)
S(1)–C(8)	1.755(3)	O(2)–Mo(1)–O(4)	99.52(10)
N(1)–N(2)	1.385(3)	O(2)–Mo(1)–O(5)	78.12(8)
N(4)–C(16)	1.440(6)	O(2)–Mo(1)–N(1)	82.78(8)
C(7)–N(1)	1.295(3)	N(1)–N(2)–C(8)	114.5(2)
C(8)–N(2)	1.291(3)		

By comparing the bond distances and angles of thiosemicarbazone with the complex, it is clear that the ligand coordinates to the MoO_2^{2+} core in the deprotonated thioiminolate form because in the complex, the C(8)–S(1) bond distance is 1.755(3) Å and is nearer to C–S single bond distance [1.81 Å] than to C–S double bond distance [1.60 Å] [33]. However, it falls short of the pure C–S single bond distance. The reason for such shortening may be attributed to electron delocalization in the coordinated ligand [34]. The adjacent C(8)–N(2) bond displays a typical double bond distance [1.291(3) Å] whereas in the ligand, C(8)–N(2) bond distance is 1.342(3) Å. The C(7)–N(1) bond distance is close to the usual C=N bond length [C(7)–N(1), 1.295(3) Å]. The N–N–C bond angle of the ligand [N(1)–N(2)–C(8), 122.0(2)^o] is reduced by few degrees [N(1)–N(2)–C(8), 114.5(2)^o] on complex formation.

The rings Cg(3) and Cg(4) make a dihedral angle of 16.36(5)^o with each other. Ring puckering analysis and least square plane calculations

show that the ring Cg(2) comprising of atoms Mo(1), O(2), C(5), C(6), C(7) and N(1) is puckered with puckering amplitude Q = 0.321(2) Å and $\phi = 190.3(6)^{o}$. Fig. 8.4. shows the unit cell packing diagram of the complex viewed along '*c*' axis.

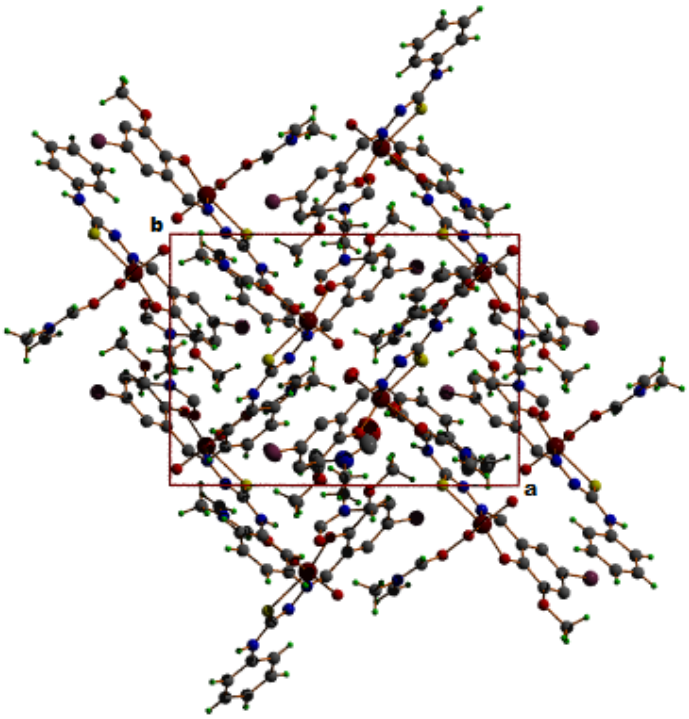

Fig. 8.4. Packing diagram of complex viewed along '*c*' axis.

A strong classical hydrogen bond N(3)–H(′)···O(6) is present in the crystal structure in which the oxygen atom of the solvent dimethylformamide acts as the acceptor (Fig. 8.5). Intramolecular and intermolecular nonclassical hydrogen bonds are also present in the crystal structure. The π···π interactions are absent while C–H···π interaction exists between H(15B) and Cg(4) comprising of atoms C(9), C(10), C(11), C(12), C(13) and C(14) (Fig. 8.6). The interaction parameters are shown in Table 8.5. The coordination polyhedra present in a super cell is shown in Fig. 8.7.

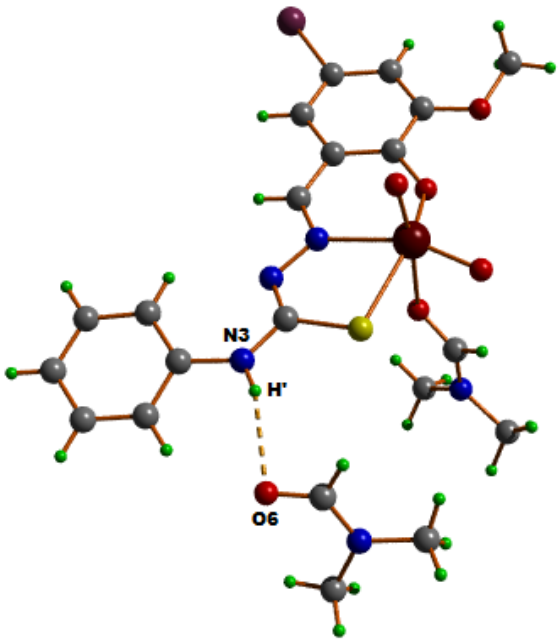

Fig. 8.5. Hydrogen bonding interaction shown as dotted line.

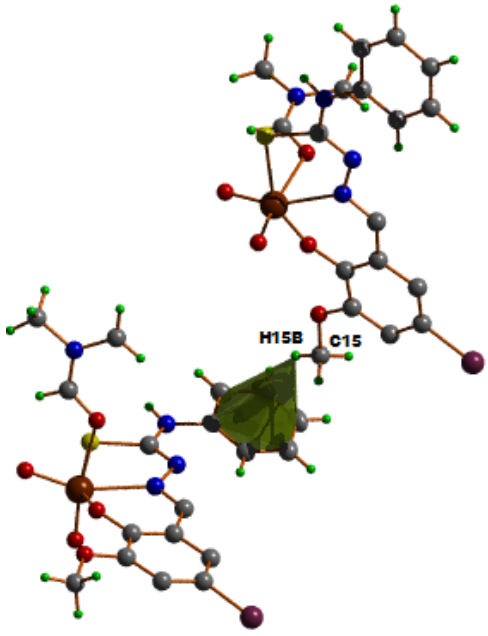

Fig. 8.6. C–H···π interactions in [MoO_2L^1DMF]·DMF (34).

Table 8.5. Interaction parameters

H-bonding				
D–H···A	**D–H (Å)**	**H···A (Å)**	**D···A (Å)**	**D–H···A (°)**
N(3)–H'···O(6)[a]	0.85(4)	2.23(3)	3.053(6)	164(4)
C(14)–H(12)···O(6)[a]	0.93	2.42	3.238(7)	147
C(12)–H(14)···N(2)[a]	0.93	2.58	3.485(5)	163
C(10)–H(16)···N(2)	0.93	2.26	2.839(4)	120
C(18)–H(21)···O(3)	0.93	2.35	2.896(5)	117
C(20)–H(30C)···O(1)[b]	0.96	2.42	3.154(9)	133
C–H···π interactions				
C–H(I)···Cg(J)	**H···Cg (Å)**	**C–H···Cg (˚)**	**C···Cg (Å)**	
C(15)–H(15B)···Cg(4)[c]	2.83	136	3.579(4)	

Equivalent position codes : a=⅔-x,½+y,½-z,b=x,y,1+z,c=-½+x,½-y, -½+z
Cg(4) = C(9), C(10), C(11), C(12), C(13), C(14)
D = Donor, A = acceptor, Cg = Centroid

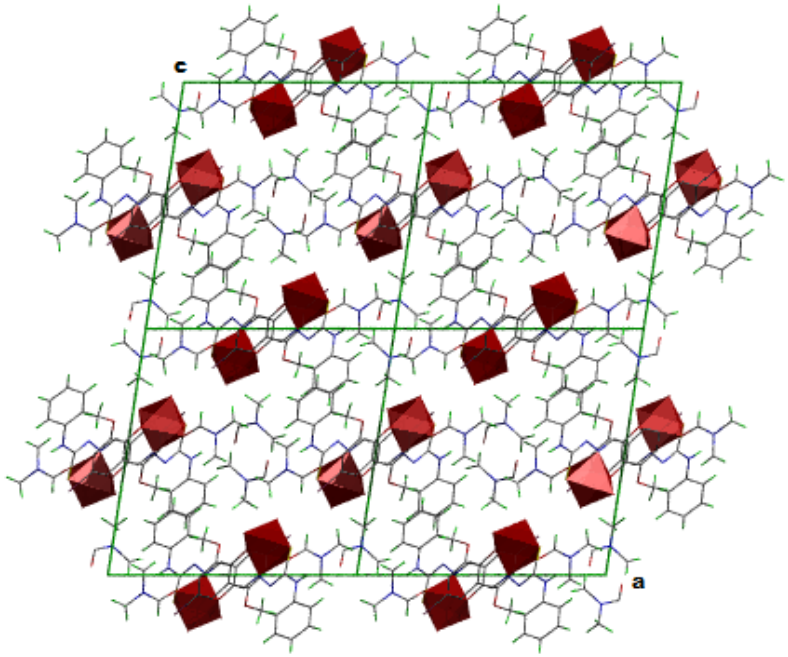

Fig. 8.7. Coordination polyhedra of $[MoO_2L^1DMF]\cdot DMF$ (34) in a super cell.

References

[1] I.K. Dhavan, J.H. Enemark, Inorg. Chem. 35 (1996) 4873.

[2] S.J.N. Burgmayer, E.I. Stiefel, J. Chem. Educ. 62 (1985) 943.

[3] R.R. Mendel, F. Bittner, Biochim. Biophys. Acta Mol. Cell Res. 1763 (2006) 621.

[4] C.D. Brondino, M.J. Romão, I. Moura, J.J.G. Moura, Curr. Opin. Chem. Biol. 10 (2006) 109.

[5] G. Hou, R. Dick, C. Zeng, G.J. Brewer, Transl. Res. 149 (2007) 260.

[6] B. Hassouneh, M. Islam, T. Nagel, Q. Pan, S.D. Merajver, T.N. Teknos, Mol. Cancer Ther. 6 (2007) 1039.

[7] H. Yanagiea, A. Ogatab, S. Mitsuib, T. Hisaa, T. Yamaseb, M. Eriguchia, Biomed. Pharmacother. 60 (2006) 349.

[8] T. Yamase, Mol. Eng. 3 (1993) 241.

[9] M. Cindrić, T. Kajfez Novak, S. Kraljević, M. Kralj, B. Kamenar, Inorg. Chim. Acta 359 (2006) 1673.

[10] P. Ghosh, O.J. D'Cruz, R.K. Narla, F.M. Uckun, Clin. Cancer Res. 6 (2000) 1536.

[11] S.B. Kumar, M. Chaudhury, J. Chem. Soc., Dalton Trans. (1992) 269.

[12] W.J. Geary, Coord. Chem. Rev. 7 (1971) 81.

[13] O.A. Rajan, A. Chakravarthy, Inorg. Chem. 20 (1981) 660.

[14] M. Joseph, V. Suni, M.R.P. Kurup, M. Nethaji, A. Kishore, S.G. Bhat, Polyhedron 23 (2004) 3069.

[15] M.A. Ali, M.T.H. Tarafdar, J. Inorg. Nucl. Chem. 39 (1977) 1785.

[16] M.J.M. Campbell, Coord. Chem. Rev. 15 (1975) 279.

[17] B.S. Garg, M.R.P. Kurup, S.K. Jain, Y.K. Bhoon, Transit. Met. Chem. 13 (1988) 247.

[18] B.S. Garg, M.R.P. Kurup, S.K. Jain, Y.K. Bhoon, Transit. Met. Chem. 16 (1991) 111.

[19] A. Syamal, K.S. Kale, Inorg. Chem. 4 (1965) 867.

[20] B.S. Garg, M.R.P. Kurup, S.K. Jain, Y.K. Bhoon, Transit. Met. Chem. 13 (1988) 309.

[21] L.J. Willis, J.M. Loehr, K.F. Miller, A.E. Bruce, E.I. Stiefel, Inorg. Chem. 25 (1986) 4289.

[22] M. Joseph, M. Kuriakose, M.R.P. Kurup, E. Suresh, A. Kishore, S.G Bhat, Polyhedron 25 (2006) 61.

[23] F.J. Arnaiz, R. Aguado, M.R. Podrosa, A.D. Cian, J. Fischer, Polyhedron 19 (2000) 2141.

[24] A. Rana, R. Dinda, P. Sengupta, L.R. Falvello, S. Ghosh, Polyhedron 21 (2002) 1023.

[25] S. Purohit, A.P. Koley, L.S. Prasad, P.T. Manoharan, S. Ghosh, Inorg. Chem. 28 (1989) 3735.

[26] C.S.J. Chang, J.H. Enemark, Inorg. Chem. 30 (1991) 683.

[27] S. Gupta, A.K. Barik, S. Pal, A. Hazra, S. Roy, R.J. Butcher, S.K. Kar, Polyhedron 26 (2007) 133.

[28] SMART and SAINT, Area Detector Software Package and SAX Area Detector Integration Program, Bruker Analytical X-ray; Madison, WI, USA, 1997.

[29] SADABS, Area Detector Absorption Correction Program; Bruker Analytical X-ray; Madison, WI, USA, 1997.

[30] G.M. Sheldrick, Acta. Cryst. A64 (2008) 112.

[31] G.M. Sheldrick, SHELXL97 and SHELXS97, University of Göttingen, Germany, 1997.

[32] K. Brandenburg, Diamond Version 3.2g, Crystal Impact GbR, Bonn, Germany, 2010.

[33] E.B. Seena, B.N. Bessy Raj, M.R.P. Kurup, E. Suresh, J. Chem. Cryst. 36 (2006) 189.

[34] M.W. Bishop, J. Chatt, J.R. Dilworth, M.B. Hursthouse, M. Motevalli, J. Chem. Soc., Dalton Trans. (1979) 1603.